

## FLOW SIMULATION AT SHOCK WAVE TRIPLE POINT

PIOTR DOERFFER<sup>1</sup>, KRYSZYNA NAMIEŚNIK<sup>1</sup>  
AND FRANCO MAGAGNATO<sup>2</sup>

<sup>1</sup>*Institute of Fluid Flow Machinery,  
Polish Academy of Sciences,  
Fiszera 14, 80-952 Gdansk, Poland  
doerffer@imp.gda.pl, knam@imp.gda.pl*

<sup>2</sup>*Fachgebiet Stroemungsmaschinen,  
Kaiserstr. 12, D-76-128 Karlsruhe, Germany  
magagnato@mach.uni-karlsruhe.de*

(Received 20 July 2001)

**Abstract:** The paper presents supersonic flow simulation results concerning the  $\lambda$ -foot formation in the divergent nozzle. The SPARC code was used and the vicinity of the triple point was analysed. Special boundary conditions have been used in order to obtain supersonic inlet velocity with shock wave in the divergent nozzle. It was proved that the condition of pressure equality on both sides of shear layer following the triple point for flow parameter of interest, does not hold.

**Keywords:** transonic flow, shock wave,  $\lambda$ -foot

### 1. Introduction

The  $\lambda$ -foot structure is created in a supersonic flow as a result of interaction between a normal shock wave and a boundary layer, see Figure 1. In the boundary layer there is a region of subsonic flow in the direct vicinity of the wall. In this region the shock wave cannot exist and therefore the pressure jump generated by the shock is spread upstream and downstream. Pressure increase at the wall, which generates a compression wave, precedes the location of the main shock wave and provokes the creation of an oblique shock wave. The compression wave coincides with the normal wave at some distance from the boundary layer. At the crossing point this wave is divided into the main and rear branches. As a result, the  $\lambda$ -foot comprises three branches: the main shock wave, the compression wave having the form of a weak oblique wave, and the strong rear branch.

The topography of the  $\lambda$ -foot is sketched in Figure 1.

The point where the three branches cross bears the name of a triple point. The  $\lambda$ -foot is mostly generated beyond the boundary layer, *i.e.* in the region where viscous effects can be neglected. Therefore, as the first approximation, the formation of the  $\lambda$ -foot can be studied using an oblique shock wave theory. As a consequence of that simplification, points 1 and 2 in Figure 1 converge to one point and the front compression is reduced to

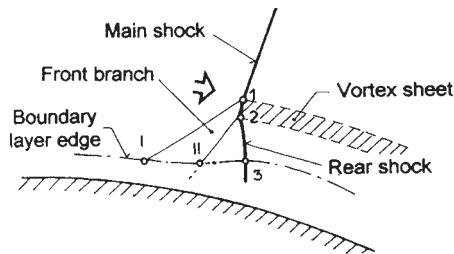


Figure 1. Sketch of a  $\lambda$ -foot topography

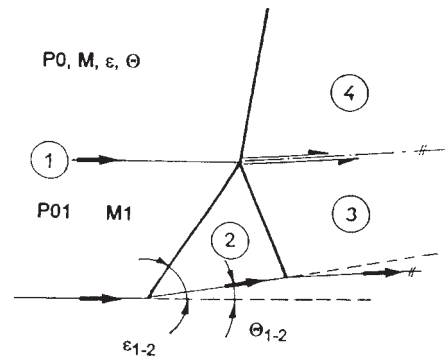


Figure 2. Flow model at the triple point

a weak-type oblique shock wave. The rear branch of the  $\lambda$ -foot is a strong-type oblique shock wave.

Figure 2 shows schematically the flow past the triple point in terms of the theory of oblique shock waves.

The flow is from left to right. The parameters of the approaching flow “1” and the stream deflection angle  $\theta_{1-2}$  are given. Those data define explicitly flow parameters in region “2”. In order to find the flow parameters downstream of the main shock wave and rear limb of the  $\lambda$ -foot, additional conditions are to be assumed for the boundary between regions “3” and “4”. Usually they are: equal static pressures and flow directions on both sides of the vortex sheet.

A convenient practice is to search the solution with the aid of the method of polar lines in the static pressure – stream deflection angle co-ordinate system. Those cases in relation to Mach number and stream deflection angle are discussed in detail in [1].

The oblique shock theory gives the solution within limited velocity and stream deflection angle ranges at the assumptions mentioned above. For very small Mach numbers (lower than 1.3) there is no solution. For higher velocities the model returns solutions corresponding to three different physical phenomena. A schematic of those solutions is given in Figure 3.

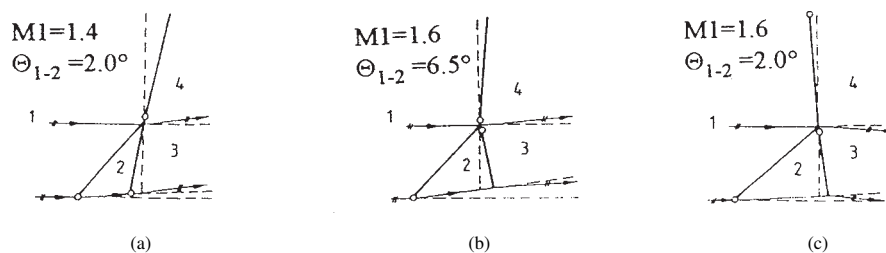


Figure 3. Three types of solution

The case in Figure 3a is typical of low Mach numbers. The flow deflection at the rear  $\lambda$ -foot shock is inclined in the same direction as at the front shock, and the general deflection in the sketch is upwards. The origin of the front and rear shock is located away from the triple point. Only the main shock originates at the triple point. Therefore this case

corresponds to the case of two oblique shocks merging into one. The case in Figure 3b corresponds to higher Mach numbers and small deflection angles. The deflection at the rear shock (downwards) is in a different direction than at the front shock. As a consequence, the rear and main shocks originate at the triple point. This case corresponds to the  $\lambda$ -foot structure. The case in Figure 3c appears at even higher Mach numbers. This time the  $\lambda$ -foot shock system deflects the stream downwards. The front shock and the main shock take their origin away from the triple point and only the rear shock originates at the triple point. This case concerns the crossing of weak and strong-type shock, which may happen at the interference of the strong oblique shock with the wall.

The condition of equal pressures and flow directions determines parameters corresponding to the system of waves from Figure 3a, while the wave pattern recorded in the experiment corresponds to the situation shown in Figure 3b. Therefore the equality condition for static pressures and flow directions on the two sides of the vortex sheet downstream of the triple point seems to be not valid in the examined case. In [1] a model has been proposed in which the equality of pressures is dropped. The same direction of flow downstream of the shock wave system results from assumed equal perpendicular components of momentum on both sides of the shear layer.

## 2. Flow geometry and boundary conditions

The validity of the conditions assumed in the modified model [1] has been investigated numerically with Navier-Stokes solver SPARC [2]. The value of such a numerical test is backed up by the fact that experimental studies of the flow in the vicinity of the shock wave are extremely difficult.

The effect of viscosity on the solution was examined by comparing results obtained for laminar, inviscid, and turbulent solutions, in the last case the  $k$ - $\tau$  model of Speziale was applied. Two numerical schemes: Slip and Switch were used in the computations [3].

Generally, in a numerical simulation we try to model the situation shown in Figure 2 as precisely as possible, assuming that the flow upstream of the wave system is uniform. This assumption is impossible to be kept in practice, as in the uniform flow the location of the shock wave is not clearly defined. Therefore in the present numerical experiment the flow channel has the form of a symmetrical divergent nozzle with a small opening angle ( $1.877^\circ$ ). As a consequence, slight non-uniformity of the flow upstream of the shock wave is obtained. In such a nozzle a straight shock wave is generated at certain inlet/exit static pressure drop characterising the supersonic flow. In order to generate a  $\lambda$ -foot, a wedge with opening angle of  $5^\circ$  is located on the lower nozzle wall. When the flow passes the wedge, it generates an oblique shock wave. The interaction of this wave with the main shock provokes the formation of the  $\lambda$ -foot structure. The geometry is shown in Figure 4 along with the numerical grid.

This is a 2D grid with maximum cell number equalling  $241 \times 129$ . SPARC makes use of a multigrid method, and Figure 4 shows, for simplicity, a coarse grid. In the region of expected  $\lambda$ -foot the grid has been condensed.

The following boundary conditions were assumed: inlet stagnation parameters (pressure and temperature), properly selected outlet static pressure (prescribed shock location), and the symmetry condition for the two remaining walls, so as not to generate a boundary layer. Since the flow is supersonic from the very inlet to the channel, the velocity condition

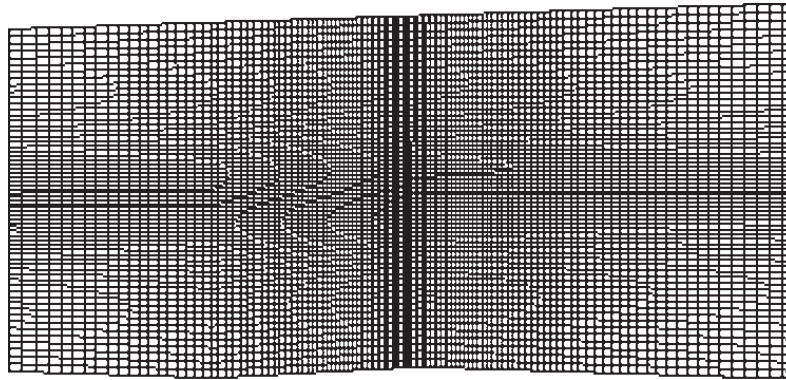


**Figure 4.** Numerical grid on the fourth level of multigrid (121×65)

has also been imposed. The value of velocity is constant, tangential to the walls, and the angle changes linearly to the centre of the nozzle. For such a condition, the inlet Mach number can be imposed and the location of the shock wave can be controlled by proper selection of the outlet static pressure.

Two following cases were studied to which the model of  $\lambda$ -foot did not apply:

- (a) Mach number  $Ma = 1.37$  upstream of the triple point (at inlet 1.2),
- (b) Mach number  $Ma = 1.7$  upstream of the triple point (at inlet 1.6).

### 3. Discussion of results

#### 3.1. Flow structure

The structure of the  $\lambda$ -foot for the two cases examined is shown in Figure 5.

Noticeable is the difference in the structure of the  $\lambda$ -foot at different velocities. The heights of the  $\lambda$ -feet are different. For higher velocity, the main shock wave upstream of the triple point is inclined in such a way that its location at the upper nozzle wall precedes the location of the triple point. Such an inclination is typical of the reflection from the wall, of the strong-type oblique shock wave (case shown in Figure 3c) rather than of a  $\lambda$ -foot. This problem needs further investigations.

Figure 6 shows the distributions of the  $\theta$  angle in four longitudinal sections in the nozzle. Figure 6a refers to  $Ma = 1.37$  upstream of the triple point, while Figure 6b – to  $Ma = 1.7$ .

Two distributions represented by black and red lines refer to the area below of the triple point. The local maximum (plateau) refers to the area between the waves of the  $\lambda$ -foot. Green and blue lines refer to the nozzle area above the triple point. It is noteworthy that the streams passing the main shock wave deflect in different directions, in Figure 6a it is the direction upwards while in Figure 6b – downwards. The angles recorded downstream of the  $\lambda$ -foot in the vicinity of the triple point (labelled with A in Figure 6a) reveal that the exit direction equals, approximately, half of the stream deflection angle on the wedge (front compression wave). In this particular case,  $Ma = 1.37$ , this corresponds to the difference in static pressures between regions “3” and “4”. This effect is better visible in Figure 10.

The presented distributions validate the assumption on equal directions of the flows leaving the triple point at the angle equal to the half of the wedge angle.

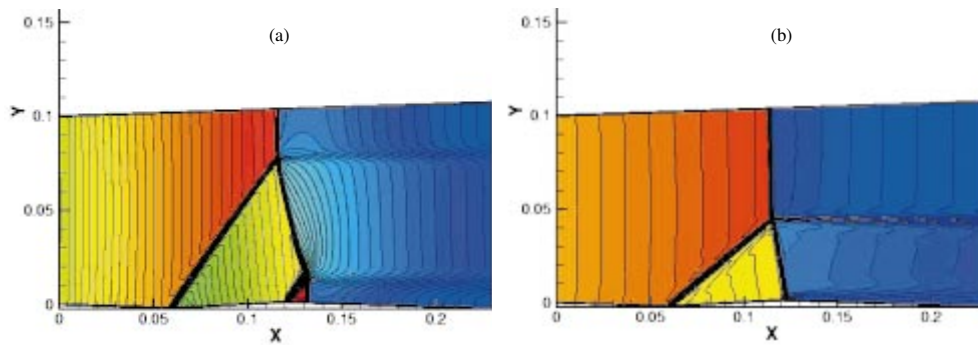


**Figure 5.** Mach isolines in the nozzle with wedge: (a)  $Ma = 1.37$  in front of the triple point; (b)  $Ma = 1.7$  in front of the triple point

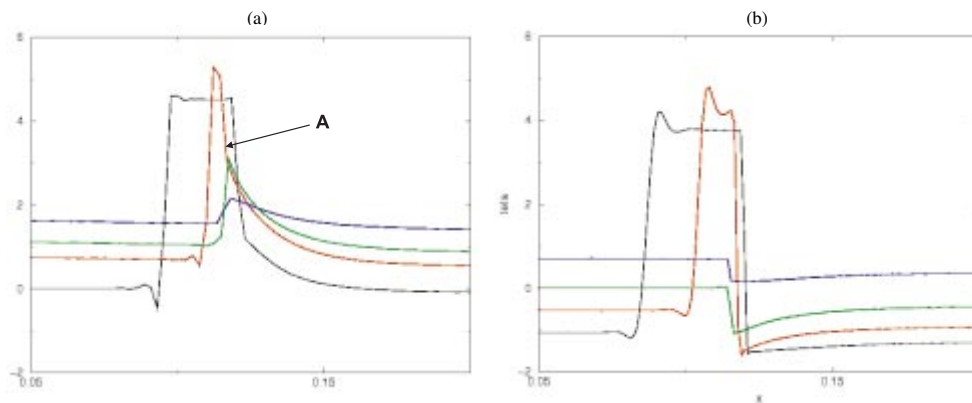


**Figure 6.** Streamwise variation of  $\theta$ -angle at four heights in the nozzle

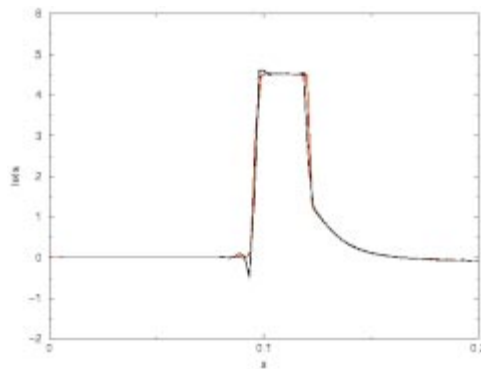


**Figure 7.** Variation of  $\theta$ -angle using Switch and Slip schemes

### 3.2. Effect of numerical scheme

Distributions of lines in Figure 6 exhibit disturbances appearing before rapid change of  $\theta$ . They are of pure numerical nature, which is confirmed by the behaviour of another numerical scheme applied, namely the Slip scheme, as opposed to the numerical scheme Switch used earlier. It is noticeable in Figure 7, presenting changes of  $\theta$ , obtained using the schemes Switch (black line) and Slip (red line), for a selected nozzle section located below

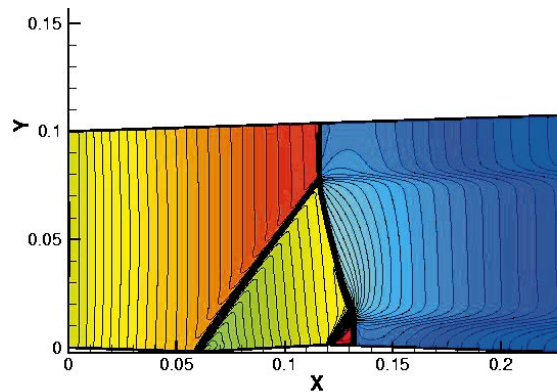


Figure 8. Mach isolines for  $Ma = 1.37$  (Slip scheme)

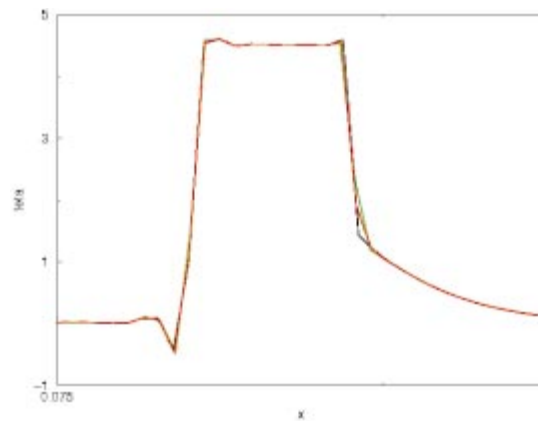


Figure 9. Comparison between turbulent, laminar, and inviscid flows

of the triple point. The solution obtained with the aid of the Slip scheme required slightly lower static pressure at the nozzle outlet than for the Switch scheme.

The comparison of the two schemes shows that the Slip scheme has different dissipation near shock waves than the Switch scheme. Due to this fact, the grid in area of  $\lambda$ -foot should present much higher density for the Slip scheme, otherwise the damping is too large (extrema cannot be caught so easily). Because of this, the number of grid points near the shock wave for the Slip scheme should be very high. The Switch scheme seems more advisable, because it gives more accurate results, for the considered grid resolution for the flows with shock waves.

The Slip scheme reveals lower gradients of parameters at waves. Observed for switch scheme overshoots result from improved shock capturing ability and steeper gradients.

Figure 8 illustrates the solution for  $Ma = 1.37$  obtained with the aid of the Slip scheme.

As was expected, the distribution of Mach number isolines is smoother here than that shown in Figure 5a, particularly in the area upstream of the front wave of the  $\lambda$ -foot.

### 3.3. Effect of physical model

The effect of a selected physical model on the nature of the obtained solutions was examined. Like in previous cases,  $\theta$  changes for a selected longitudinal section of the nozzle

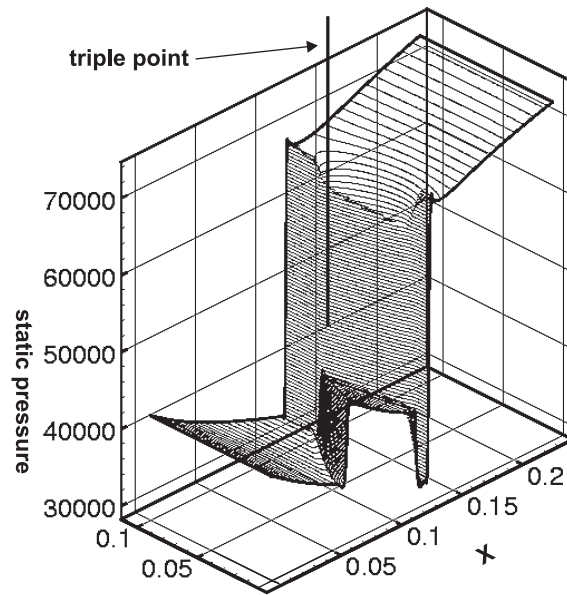


Figure 10. Static pressure gradient in the nozzle (Ma = 1.37)

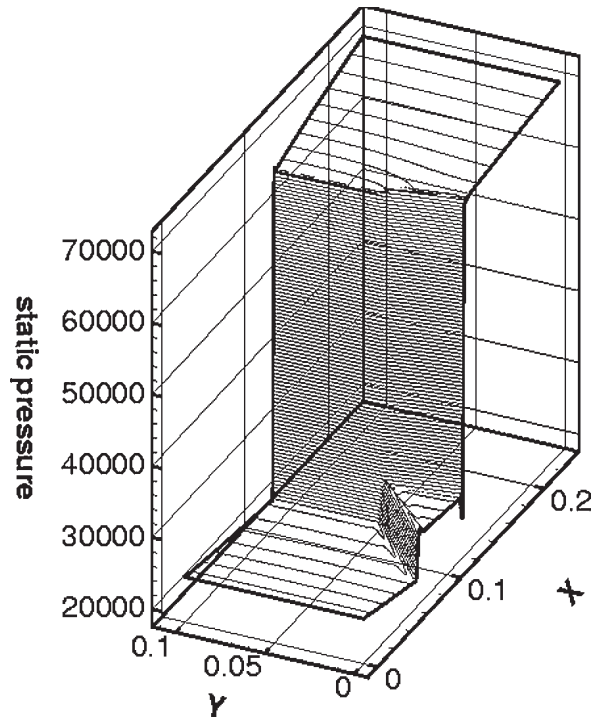


Figure 11. Static pressure gradient in the nozzle (Ma = 1.7)

were examined in relation to the type of flow. Figure 9 presents three curves: the black line corresponds to the turbulent flow, red line – to the inviscid flow, while the green line – to the laminar flow.

There is no practical difference between distributions of parameters for all three types of flow. This meets the expectations as the  $\lambda$ -foot is generated beyond the boundary layer, in the inviscid flow region.

The effect of the physical model on the solution was also examined by traversing perpendicularly the nozzle at two sections: near the triple point (at, approximately, 3 cm downstream) and at the nozzle exit (at about 15 cm downstream of the triple point).

Total pressure distributions were analysed in those sections, especially in the wake downstream of the triple point. The wake in this area is of convection nature. Particles which take part in the shear layer move downstream with the stream velocity. Therefore the turbulence had been expected not to have significant impact on the shear layer profile. The results of the simulations obtained for inviscid, laminar, and turbulent flows do not exhibit differences in the distributions of flow parameters, which confirms the hypothesis concerning the absence of turbulence effect on the stream downstream of the triple point, at least at such a short streamwise distance as that examined in the simulation.

Of certain interest are the obtained static pressure distributions in the channel. Figure 10 refers to lower, while Figure 11 – to higher velocity flow.

The figures reveal a noticeable jump of static pressure across the shock wave. In both cases a  $\lambda$ -foot is created. Downstream of the triple point, a transverse gradient of the static pressure is created on both sides of the vortex sheet. This gradient is high for  $Ma = 1.37$  and disappears downstream of the wave, in the region of subsonic flow. For  $Ma = 1.7$  the static pressure observed downstream of the  $\lambda$ -foot is higher than downstream of the main wave. In this case the pressure gradient has opposite direction. Those figures confirm the validity of the assumption of different static pressures downstream of the  $\lambda$ -foot on both sides of the vortex sheet.

#### 4. Conclusions

The results of the numerical simulation of the flow with the  $\lambda$ -foot structure in a nozzle can be summed up in the following conclusions:

1. In the process of formation of shock wave structure at the triple point, the equality of static pressures on the two sides of the vortex sheet is not a necessary condition.
2. Flow directions downstream of the triple point are identical at both sides of the wake.
3. The development of the aerodynamic wake downstream of the triple point does not exhibit the effect of turbulence in the examined area.
4. In spite of overshoots in the vicinity of shock waves, the Switch scheme is more advisable due to lower requirements concerning mesh resolution and better physical agreement with experiment.

#### References

- [1] Doerffer P 1994 *Acta Mechanica* pp. 133–140
- [2] Magagnato F 1998 *Task Quarterly* **2** (2) 215
- [3] Tatsumi S, Martinelli L and Jameson A 1995 *J. AIAA* **33** (2) 252